Geomechanics and Engineering, *Vol. 33, No. 1 (2023) 113-120*
https://doi.org/10.12989/gae.2023.33.1.113

Compressibility of fine-grained sediments based on pore water salinity changes

Junbong Jang* and Handikajati Kusuma Marjadi[a]

Department of ICT Integrated Safe Ocean Smart Cities Engineering, Dong-A University, Busan 49315, South Korea

(*Received November 28, 2022, Revised March 14, 2023, Accepted March 16, 2023*)

Abstract. Coastal and offshore structures such as ports and offshore wind farms will often need to be built on fine-grained sediments. Geotechnical properties associated with sediment compressibility are key parameters for marine construction designs especially on soft grounds, which involve clay-mineral dominated fines that can consolidate and settle significantly in response to engineered and environmental loads. We conduct liquid limit tests and 1D consolidation tests with fine-grained soils (silica silt, mica, kaolin and bentonite) and biogenic soils (diatom). The pore fluids for the liquid limit tests include deionized water and a series of brines with NaCl salt concentrations of 0.001 m, 0.01 m, 0.1 m, 0.6 m and 2.0 m, and the pore fluids for the consolidation tests deionized water, 0.01 m, 0.6 m, 2 m. The salt concentrations help the liquid limits of kaolin and bentonite decrease, but those of diatom slightly increase. The silica silt and mica show minimal changes in liquid limit due to salt concentrations. Accordingly, compression indices of soils follow the trend of the liquid limit as the liquid limit determined the initial void ratio of the consolidation test. Diatoms are more likely to be broken than clastic sediments during to loading, and diatom-rich sediment is therefore generally more compressible than clastic-rich sediment.

Keywords: fine-grained soils; electrical forces; liquid limit; pore-fluid chemistry; soil classification

1. Introduction

Coastal cities have more than 50% of world population (Barragan and Andres 2015) while the coastal areas are much smaller than the inland areas. In order to develop coastal cities such Busan in South Korea, structures such as ports and bridges would be located near ocean. We easily find fine-grained sediments near coastal areas, and most of marine sediments are fine-grained sediments because of sediment erosion and transport (Kennett 1982). We should utilize fine-grained sediments, which usually show high compressibility, low permeability and low shear strength (Mitchell and Soga 2005). Fine-grained sediments may be unsuitable conditions for structures and can cause unstable conditions. High compressible, weak fine-grained sediments can be considered soft ground on where constructions induce large settlement during engineering applications. The ground improvement methods such as deep cement mixing and preloading with vertical drains can be required to control compressibility and shear strength (Ali *et al*. 2020, Choo *et al*. 2020, Han 2015, Shariati *et al*. 2020, Yu *et al*. 2020).

Compressional behavior of fine-grained sediments consists of elastic and plastic settlements (Leonards and Altschaeffl 1964, Taylor 1948). Both settlements can occur simultaneously after loading, but most settlements of total settlements of fine-grained sediments are due to plastic settlements including consolidation and creep. Not only large long-term settlements but also non-uniform settlements jeopardize structures (Fattah *et al*. 2013). One of famous non-uniform settlement cases is the Leaning Tower of Pisa, and the ground remediation controlled continuous settlement (Burland *et al*. 2002). Many structures on coastal areas should avoid damages by non-uniform settlements.

Fine-grained sediments are silt- (particle size less than 75μm) or clay-sized (particle size less than 2 μm) sediments (ASTM D2487, 2011). Because of small particles sizes, the particle arrangement or fabric is influenced by electrical forces between particles (Jang *et al*. 2018, Lambe and Whitman 1969, Santamarina *et al*. 2001, Won *et al*. 2021). Nano-size particles can float or accumulate as a cluster in water as the ions in the fluid neutralize the electrical repulsion between particles and that can allow particles to flocculate together even though the particles are non-clay minerals (McBride and Baveye 2002, Sogami and Ise 1984)

Particle shape and mineralogy can affect soil fabrics. Platy fine grains of clay minerals are sensitive to pore fluid chemistry (Jang *et al*. 2018, Mitchell and Soga 2005). Platy fine grains with unbalanced surface charges of clay mineral grains such as kaolinite and montmorillonite may form fabrics dominated by electrical interactions such as face-to-face and edge-to-face depending on ionic concentrations in pore fluid. The permittivity and ionic concentrations affect interparticle forces (F) between the grains in water based on Coulomb's law.

$$F = \frac{1}{4\pi\epsilon_0}\frac{q_1 q_2}{r^2} \quad (1)$$

*Corresponding author, Assistant Professor
E-mail: jjang@dau.ac.kr
[a]Ph.D. Student

Copyright © 2023 Techno-Press, Ltd.

ISSN: 2005-307X (Print), 2092-6219 (Online)

where the q_1 and q_2 are the two charges, ϵ_0 the vacuum permittivity, r the distance between two charges (Young and Fredman 2004). Also, the diffusive double layer (DDL) on clay mineral particles appears and affects particle arrangement. The DDL thickness (ϑ) can be estimated below.

$$\vartheta = \sqrt{\frac{\epsilon_0 R}{2F^2}\frac{\kappa' T}{c_0 z^2}} \quad (2)$$

where R is the gas constant, 8.314J/(K·mol), F the Faradays' constant, 9.6485×104C/mol, κ' the permittivity of pore fluid, T the temperature, c_0 the bulk fluid ionic concentration, and z the ion valence (Israelachvili 2011, Santamarina *et al.* 2001).

Derjaguin-Landau-Verwey-Overbeek (DLVO) theory can predict electrical interactions with van der Waals attraction (F_{att}) and DDL repulsion (F_{rep})of thin clay-sized clay mineral particles such as montmorillonite particles due to ionic concentration changes (Israelachvili 2011, Santamarina *et al.* 2001, Verwey *et al*. 1948)

$$F_{att} = -\frac{A_h}{6\pi r^3} \quad (3)$$

$$F_{rep} = 64RTc_0 e^{-r/\vartheta} \quad (4)$$

where A_h is Hamaker constant. The electrical interactions introduced in Eqs. (1) to (4) can govern the grain arrangement or fabric of fine-grain soils, and the fabric affect the liquid limit and compressibility of remolded fines (Burland 1990, Cerato and Lutenegger 2004, Jang and Santamarian 2015, Won *et al.* 2021).

In general, experiments for the liquid limit tests such as cone-penetrometer test and Casagrande cup method use remolded specimens, and the consolidation test with remolded specimens can follow. The liquid limits and compression indices of remolded samples are highly related (Onyejekwe *et al.* 2015, Tiwari *et al.* 2012). Remolded samples have no geological history such as diagenesis and preconsolidation stress (Ballas *et al.* 2018, Schmertmann 1991). Soil fabric and pore fluid would resist to the vertical stress, and soils with high void ratio produce more compressibility. Eqs. (1) to (4) indicate that the permittivity and ionic concentration in bulk fluid or pore fluid affect the electrical interactions between grains and lead to different fabrics. Also, the charges on grains surfaces based on mineralogy can affect the electrical forces and electrical-force-dominated fabrics. Thus, we conducted liquid limit tests and consolidation tests with different ionic concentrations using natural sediments to see how the endmember soils behave in different ionic concentrations.

2. Experimental methods

Fine-grained endmember soils in this study are silica silt, mica, diatoms (microfossils of diatom skeletons), kaolin, and bentonite to represent bulky/platy shapes, clastic/biogenic origins, clay/non-clay minerals, and interpore/intrapore particles (Table 1).

Fig. 1 provides SEM images of individual grains of the endmember soils. The bentonite adsorbed the moisture in air and become accumulated lumps. Physical properties such as specific surface area, specific gravity, and grain sized distribution were measured (See details in Jang *et al*. 2018). In order to change ionic concentrations, we used NaCl salt in water. The pore fluids for the soil materials were deionized-water (DW) and brines of NaCl solutions from low to high salinities: 0.001 m (molality, mol/kg), 0.01 m, 0.1 m, 0.6 m, and 2 m.

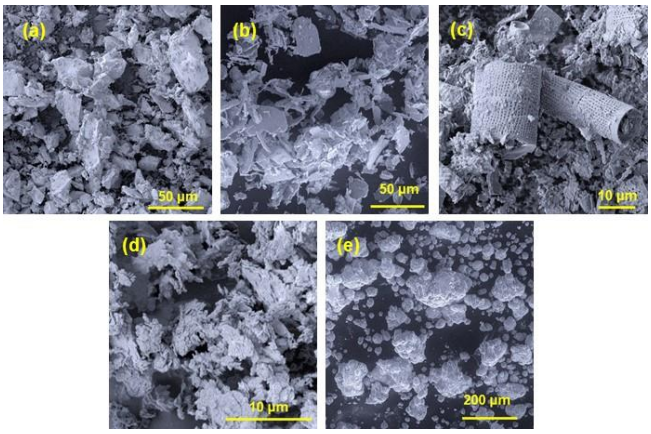

Fig. 1 Endmember soils: (a) silic silt, (b) diatoms, (c) mica and (d) bentonite

Table 1 Morphology and mineralogy of endmember soils

endmember soils	bulky or platy	clastic or biogenic	clay or non-clay mineral
silica silt	bulky	clastic	non-clay
mica	platy	clastic	non-clay
diatoms	bulky (inner-porosity)	biogenic	non-clay
kaolin	platy	clastic	clay (1:1 clay mineral)
bentonite	platy	clastic	clay (2:1 clay mineral)

The liquid limit (LL) at different salinities can show fabric changes in uniformly mixed soils (Jang *et al*. 2018). We conducted liquid limit tests using cone-penetrometer test (BS 1377, 1990). The sample was mixed with pore fluid at low water content and stayed one day to homogenize the moisture. The sample was packed in the brass sample tin as dense state to minimize the density variation of the sample in the tin. The liquid limit test was conducted from dry to wet condition to maintain the target salinity.

We used the liquid limit data to prepare samples for 1D incremental loading consolidation tests (ASTM D2453, Burland 1990). The initial water content of the sample for consolidation test was 120% of the liquid limit that was corrected by salt concentration in the pore fluid (ASTM D4524, Jang and Santamarina 2017). The control motor moves the platen up and down to control the vertical stress in the consolidation loading frame (Fig. 2). Consolidation tests follow the loading-unloading-reloading sequence between 20 kPa to 1280 kPa. The load cell and the LVDT (linear variable differential transformer) record the vertical

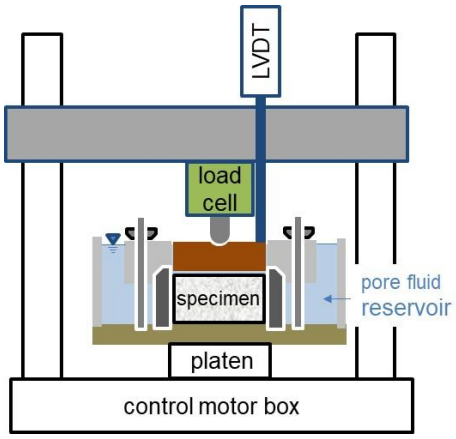

Fig. 2 Experimental configuration of consolidation tests

Table 2 Physical and index properties of endmember soils

endmember soils	d_{50} [μm]	S_s [m²/g]	liquid limit	
			LL_{DW}*	LL_{2m}*
silica silt	10.5	0.2	31	31
mica	4.2	94	94	81
diatoms	10	98	119	111
kaolin	4	24	77	55
bentonite	< 2	579	288	126

*LL_{DW} is liquid limit with deionized water and LL_{2m} liquid limit with 2m-brine

force and the vertical displacement. The specimen size is 63.5 mm(2.5in) diameter and 25.4 mm (1in) height.

3. Results

Physical properties of the soils were presented in Table 2 (also see Jang *et al.* 2018). Median particle size (d_{50}) and specific surface area (S_s) are obtained and are related to the morphology of grains as we selected endmember soils to represent different particle shape and inner-porosity.

3.1 Liquid limit

Liquid limits of soils with different salinities are shown in Fig. 3. Changes in the liquid limits represents soil fabric change due to salt concentrations in the pore fluid without grain segregation (Jang and Santamarina 2016, Won *et al.* 2021). Kaolin and bentonite are clay minerals with thin platy shape and high specific surfaces. The liquid limits of kaolin and bentonite decrease with increases in salinity as the salt ions can reduce the diffuse double layer thickness and the repulsion between grains that form dense fabric such as face-to-face fabric and dispersed fabric. The void ratio at the liquid limit goes up when the salinity decreases. Mica is also platy and high specific surface area and the mineralogy is phyllosilicate mineral. The liquid limit of mica is non-sensitive to the salinity changes as the difference between the liquid limits with brines is less than 5%.

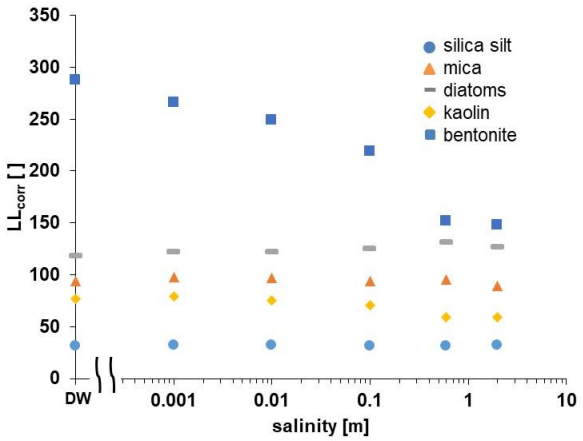

Fig. 3 Liquid limit test results at different salinity. The liquid limit corrected (LL_{corr}) is to present the water weight to solid weight without salt weight after drying (ASTM D4542, Jang and Santamarina 2017)

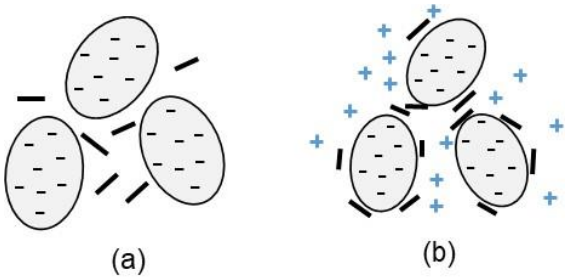

Fig. 4 Fabrics with large bulky grains (elliptical shape) and small platy grains (short-line shape): (a) large bulky grains form skeletal fabric and small grains stays in voids between the skeletal fabric in deionized water and (b) mixed fabric that small grains electrically attracted on large grains are involved large grain contacts in brine (the cross-shape means cations)

The mineralogy of silica silt and diatoms is silicate, the compound of silicon and oxygen. The liquid limits of silica silt are non-sensitive to salinity compared to platy particles and clay minerals. The diatoms show slightly sensitive to salinity as the difference between the liquid limits are less than 10%. The liquid limit increases with the salinity. This increase may be attributed that the fabric mixed with skeletal contact and fine-grain-contact between grains in brines (Fig. 4).

3.2 Consolidation

The void ratio and stress (*e-logσ'*) curves from consolidation tests are presented in Fig. 5. The initial void ratios are related to the liquid limits and its fabric without vertical loads, and consequently affect the compressional curves. The covers at different salinities tend to merge at the maximum vertical stress, 1028 kPa as the mechanical stress overcomes the electrical interparticle interactions. Salt concentration Compression index (C_c) and recompression index (C_r) are evaluated by Eq. (5) and summarized in Fig. 6.

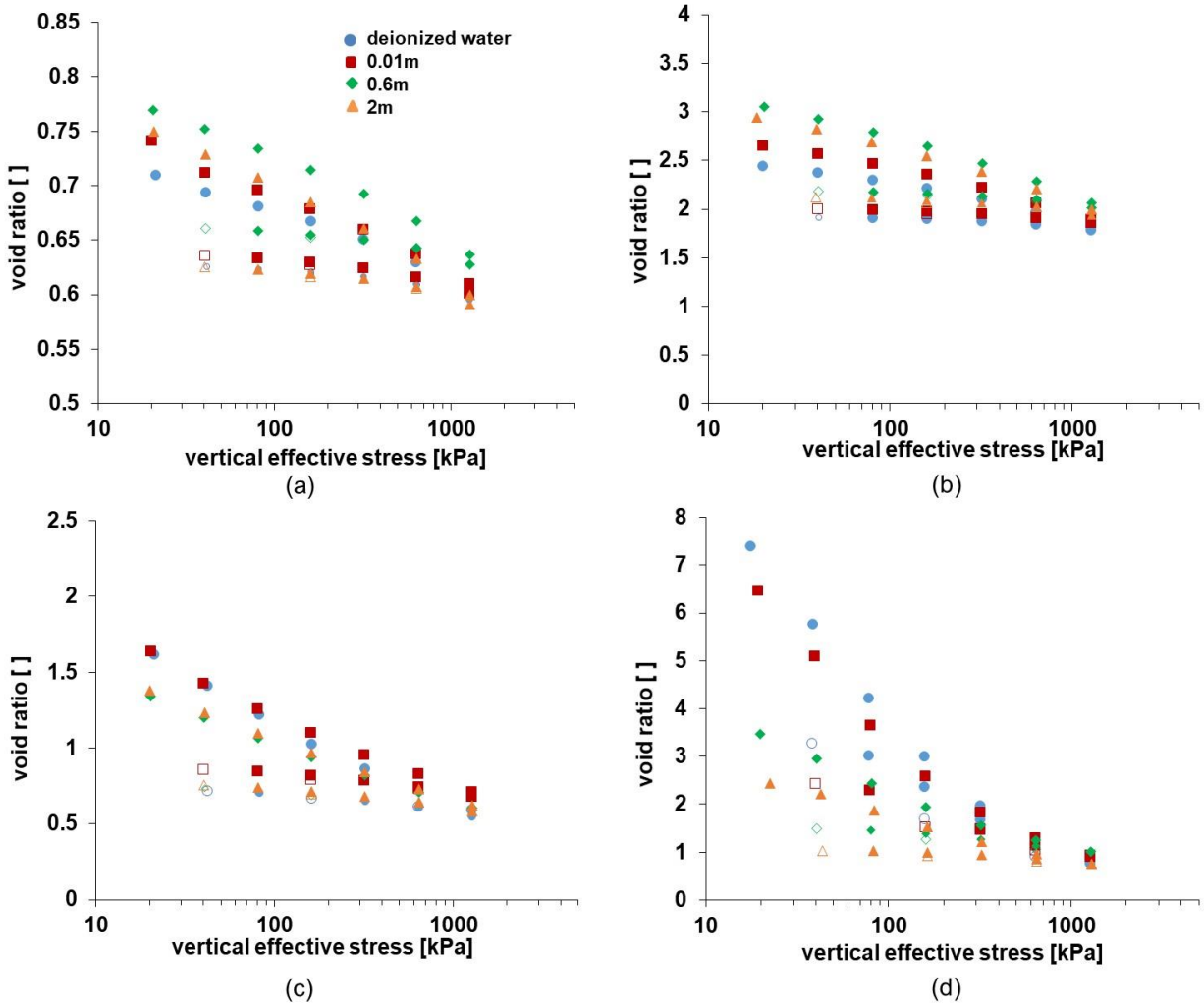

Fig. 5 Void ratio and stress (*e-logσ'*) curves from consolidation test results: (a) silica silt (b) diatoms (c) kaolin and (d) bentonite

$$C_c or\ C_r = -\frac{e_{100kPa} - e_{1,000kPa}}{100kPa - 1{,}000kPa} \quad (5)$$

The compression indices of the silica silt and diatom go up when the salt concentration of brine increases although the increases in the compression indices of the silica silt is minimal. The silica silt and diatom are silica minerals but the silica silt is clastic and diatom biogenic. The particle shape of large particles of silica silt is bulky, but the diatom has inner-pore structure and shards of the diatom is irregular. Silica silt and diatom in deionized water would have repulsion between particles in deionized water but the repulsion can diminish as ions can neutralize the surface charge of particles in salt water based on Sogami-Ise model (Sogami and Ise 1984). Smaller particles of them in brines can attach on larger particles and that induce more compressible fabric than that of the silica silt in deionized water as smaller particles repulse the larger particles (Fig. 4). Because of the shard shapes of diatom, the diatom may show more changes in compressibility due to salt concentration.

Unlike the silica silt and diatom, the bentonite and the kaolin show less compressibility when the salinity increases. They are small platy clay minerals and induce relatively thick double layer thickness in deionized water compared to the particle thickness. The thick double layer thickness induces large compressibility in deionized water. The salt ions can reduce the DDL and that leads the decreases in compression index. Also, the kaolin can form edge-to-face fabric in deionized water, and face-to-face in brine. The edge-to-face fabric is more compressible geometrically.

The loading process destructured initial fabric and only elastic rebound between particles occurred during the unloading process. The recompression indices of the bentonite are sensitive to salt concentrations in pore fluid while silica silt, diatoms and kaolin have low recompression indices in deionized water and the brines. (Fig. 6). Only DDL of grains was able to be recovered when the external loadings were removed while other electrical interactions were irreversible. DDL of the bentonite was recovered and caused the bentonite to swell as the osmotic pressure

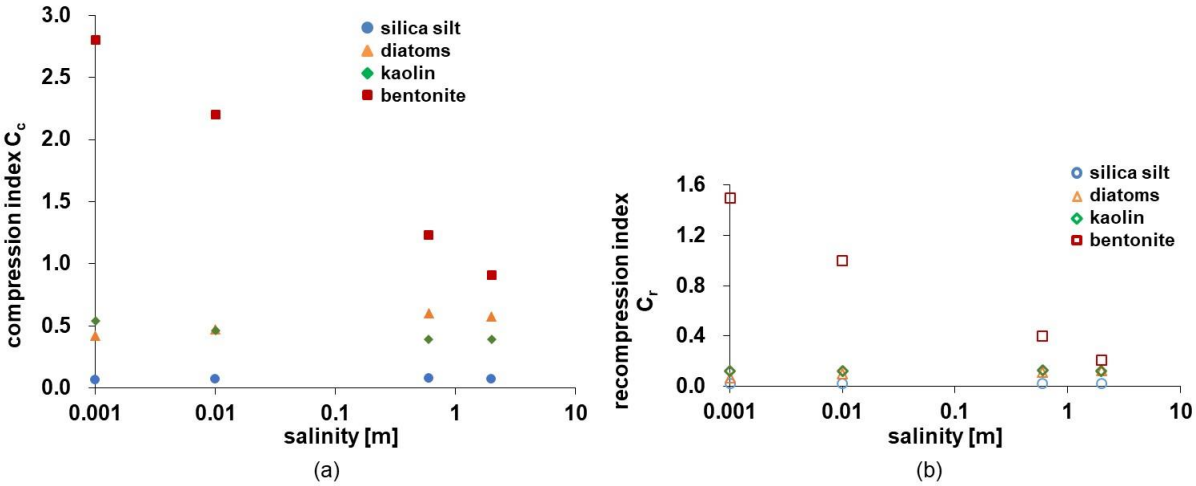

Fig. 6 (a) Compression index and (b) recompression index at different salinities

overcame the vertical stress during the unloading process (Thapa *et al.* 2020, Yang *et al.* 2021). As the DDL of bentonite shrunk due to the salt concentration, the recompression indices decreased when the salt concentration went up. The diatom, which has minimal impacts of DDL, shows increases in the recompression indices when the salt concentration increases. The shards of diatom which has inner pores and curved shapes may include elastic deformation more than that of other endmember soils.

The recompression indices of silica silt and kaolin are insensitive to salt concentration although the recompression indices of silica silt are much smaller than those of kaolin. The initial fabric formed by electrical forces was destructured and that caused the plastic deformation including primary consolidation and secondary consolidation, which were irreversible during the unloading process.

The compression index and recompression index are parameters to calculate settlements of ground. Also, we need to calculate when the consolidation would end. For consolidation time, we can calculate coefficient of consolidation (c_v) using the graphical method of the root-square-time to obtain the time at 90% degree of consolidation (t_{90}) and the time factor (T_v) by Terzaghi's consolidation theory (Taylor 1948, Terzaghi *et al.* 1996).

$$c_v = \frac{T_v t_{90}}{H_{dr}} \tag{6}$$

where the H_{dr} is the drainage distance. The coefficient of consolidation of the bentonite with the deionized water decreases from 2.71×10^{-8}m^2/s to 5.8×10^{-11}m^2/s during the loading process from low to high vertical stress. The coefficient of the consolidation would go up when the salinity in pore fluid increases. The coefficient of consolidation of the bentonite with the 2m-brine decreases from 1.13×10^{-7}m^2/s to 3.11×10^{-9}m^2/s. Also, the coefficient of consolidation of the silica silt with deionized water decreases from 1.70×10^{-6}m^2/s to 4.14×10^{-6}m^2/s and that with 2m-brine varies from 4.37×10^{-6}m^2/s. The t_{90} of the silica silt is small and hard to identify with graphical method as the silica silt has minimal consolidation behavior. Thus, the coefficients of consolidation between different salinity shows small variation.

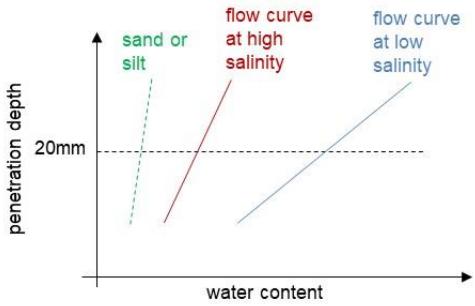

Fig. 7 Schematic drawing of flow curves from cone penetration tests that shows changes in liquid limit of high plastic soils with high electrical sensitivity such as bentonite in the brines. Green line is a reference line of non-plastic soils with low electrical sensitivity such as sand or silt

4. Discussion

4.1 Liquid limit

The liquid limit change implies how the fabric can alter due to the salinity in the pore fluid. Liquid limit is the soil consistency boundary between the plastic and liquid state, which has the undrained shear strength of approximately 2 kPa (Haigh 2012, Kayabali and Tufenkci 2010) under saturated conditions. The liquid limit of fine grains depends on mineralogy and morphology of grains due to electrical interactions with pore fluids (Jang and Santamarina 2015, Won *et al.* 2021). Accordingly, the shear strength of clayey fines would change due to the salinity. The soil morphology and mineral type of bentonite with ions can increase the undrained shear strength under saturated and confined stress conditions (Geng *et al.* 2022, Santamarina *et al.* 2002). The

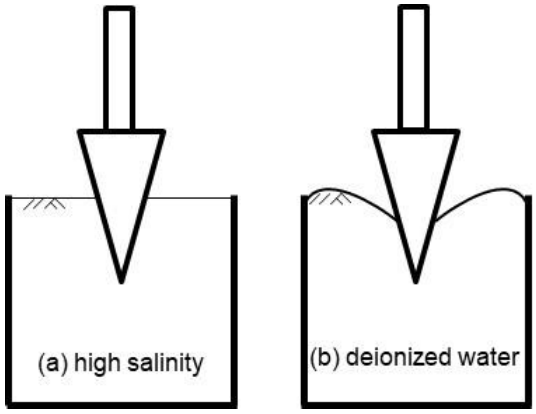

Fig. 7 Schematic drawing of flow curves from cone penetration tests that shows changes in liquid limit of high plastic soils with high electrical sensitivity such as bentonite in the brines. Green line is a reference line of non-plastic soils with low electrical sensitivity such as sand or silt

bentonite in the brines would show non-plastic behavior and low void ratio at the liquid limit (Fig. 7), and that can lead higher shear strength by triaxial tests under saturated and confined stress conditions (Mitchell and Soga 2005, Oda 1977, Zeng 2021).

Flow curves are the lines of determining the liquid limit for each sample. The flow curve slopes of bentonite become steeper when the salinity in the pore fluid increases (Fig. 7). The silica silt has steep slope of the flow curves at low water content regardless of the salinity. Although the liquid limits in the brines present minimal changes, the surface shape of the deionized water sample after the cone penetration shows significant dilation (Fig. 8). The surface deformation can easily identify which one is deionized water sample. The dilation can occur in dense granular materials (Reynolds 1886, Rowe 1962). Based on the surface deformation (Fig. 8) and fabrics with bulky grains and platy grains (Fig. 4), the deionized water sample can have denser fabric compared to the brine samples.

4.2 Consolidation

The compressibility changes due to the salt concentration based on shape and mineralogy of soil grains. The liquid limits with mixed with endmembers and different salt conditions in water changed as the electrical forces alter fabric of fine grains. Accordingly, the initial void ratio of the consolidation test at 1.2LL follows the changes of liquid limit, and the high initial void ratio induce high compression index. The correlation between compression index and recompression index of bentonite and the salt concentration is below

$$C_c = -0.246ln(c_{salt}) + 1.088 \quad (6)$$

$$C_r = -0.165ln(c_{salt}) + 0.309 \quad (7)$$

where c_{salt} is the salt concentration of pore fluid.

When two different endmembers are mixed, the compression index are interpolated between the compression indices of two endmembers. For example, in case of the mixtures of montmorillonite and quartz, the compression index of montmorillonite in deionized water is the highest value and that of quartz the lowest value, and the compression indices would exist between two values (Tiwari and Ajmera 2011). In the same manner, compression indices of the mixtures at different salt concentration could be estimated by extreme values at salt concentrations

Of particular interest offshore marine sediments, where diatom-rich sediments are common, diatoms are more likely to be broken than clastic sediments due to loading, and diatom-rich sediment is therefore generally more compressible than clastic-rich sediment. The crushing of diatoms can gradually evolve and affect the shape of the consolidation curve, contributing to the secondary consolidation or creep, which is a plastic (non-recoverable) strain. The settlement by the compressibility will reach the maximum settlement when the fabric is the densest. Although the inner-pore particles such as fly ash and microfossils may be breakable and show eccentric compressibility, they will meet terminal, minimum void ratio. When the fine-grained sediments involve clay minerals and diatoms, the compression index could be large and the consolidation by external loading can induce long-term settlements.

5. Conclusions

We studied soil fabrics and compressibility of fine-grained sediments at different salinity conducting liquid limit tests and 1D consolidation tests. Liquid limit tests can represent how homogenized soil fabric can alter due to the salinity. Based on the mineralogy, the liquid limit of silica silt and mica are non-sensitive to the salinity changes in pore fluids. The salinity in pore fluids prompts the diatoms, which have inner-pores and broken shards, to alter the liquid limits, and the kaolin and bentonite to present significant liquid limit changes. Based on the cone penetration test, the flow curve shows the how the liquid limit moves depending on the soil characteristics.

For settlement analyses, parameters of compressibility should be assessed. The compression and recompression indices are highly correlated with the liquid limits as the fabric of fine-grained soils determine the compressibility of soils. The salinity can cause fine grains of clay-minerals such as bentonite and kaolin to reduce the compression indices when the salinity increases. The recompression indices have little impacts by salinity except for the bentonite, which is a swelling clay. However, the diatoms show eccentric behavior as they are crushable and inner pore can deform elastically. When marine soils have high contents of the diatoms or microfossils, the settlement can last longer than clastic fine-grained sediments.

Acknowledgments

This work was supported by the National Research Foundation of Korea (NRF) grant funded by the Korea

government (MSIT) (No. NRF-2021R1F1A1060406). I appreciate the researchers at U.S. Geological Survey: Dr. William F. Waite provided valuable comments on the experimental results, Lee-Gray Boze helped the experiments, and Laura L. Stern took SEM images.

References

Ali, M., Aziz, M., Hamza, M. and Madni, M.F. (2020), "Engineering properties of expansive soil treated with polypropylene fibers", *Geomech. Eng.*, **22**(3), 227-236. https://doi.org/10.12989/gae.2020.22.3.227.

ASTM. (2007), "Standard Test Method for Pore Water Extraction and Determination of the Soluble Salt Content of Soils by Refractometer". ASTM D4542. ASTM International, West Conshohocken, PA.

ASTM. (2011), "Standard practice for classification of soils for engineering purposes (Unified Soil Classification System)", ASTM D2487. ASTM, West Conshohocken, PA.

Ballas, G., Garziglia, S., Sultan, N., Pelleter, E., Toucanne, S., Marsset, T., Riboulot, V. and Ker, S. (2018), "Influence of early diagenesis on geotechnical properties of clay sediments (Romania, Black Sea)", *Eng. Geol.*, **240**, 175-188. https://doi.org/10.1016/j.enggeo.2018.04.019.

Barragan, J.M. and de Andres, M. (2015), "Analysis and trends of the world's coastal cities and agglomerations", *Ocean Coast. Management*, **114**, 11-20. https://doi.org/10.1016/j.ocecoaman.2015.06.004.

Burland, J.B. (1990), "30th rankine lecture - on the compressibility and shear-strength of natural clays", *Geotechnique*, **40**(3), 329-378.

Burland, J.B., Jamiolkowshi, M. and Viggiani, C. (2003), "The stabilisation of the leaning Tower of Pisa", *Soils Found.*, **43**(5), 63-80. https://doi.org/10.3208/sandf.43.5_63.

Cerato, A.B. and Lutenegger, A.J. (2004), "Determining intrinsic compressibility of fine-grained soils", *J. Geotech. Geoenviron. Eng.*, **130**(8), 872-877. https://doi.org/10.1061/(Asce)1090-0241(2004)130:8(872).

Choo, H., Choi, Y., Kim, Y.U., Lee, W. and Lee, C. (2020), "Compressibility and hydraulic conductivity of calcium bentonite treated with pH-responsive polymer", *Geomech. Eng.*, **22**(4), 329-337. https://doi.org/10.12989/gae.2020.22.4.329.

Fattah, M.Y., Al-Mosawi, M.J. and Al-Zayadi, A.A.O. (2013), "Time dependent behavior of piled raft foundation in clayey soil", *Geomech. Eng.*, **5**(1), 17-36. https://doi.org/10.12989/gae.2013.5.1.017.

Geng, W.J., Han, W.X., Yin, J. and Lu, Z.J. (2022), "Salinity effects on the strength and morphological indices of soft marine clay", *Scientific Reports*, **12**(1). ARTN 17563. https://doi.org/10.1038/s41598-022-22627-w.

Haigh, S.K. (2012), "Mechanics of the Casagrande liquid limit test", *Can. Geotech. J.*, **49**(9), 1015-1023. https://doi.org/10.1139/T2012-066.

Han, J. (2015), "Principles and practices of ground improvement", John Wiley & Sons, Inc., Hoboken, New Jersey.

Israelachvili, J.N. (2011), "Intermolecular and surface forces", Academic Press. San Diego, CA.

Jang, J. and Santamarina, J.C. (2016), "Fines classification based on sensitivity to pore-fluid chemistry", *J. Geotech. Geoenviron. Eng.*, **142**(4), 06015018. Artn 06015018. https://doi.org/10.1061/(Asce)Gt.1943-5606.0001420.

Jang, J. and Santamarina, J.C. (2017), "Closure to "Fines Classification Based on Sensitivity to Pore-Fluid Chemistry" by Junbong Jang and J. Carlos Santamarina", *J. Geotech. Geoenviron. Eng.*, **143**(7), 07017013. Artn 07017013. https://doi.org/10.1061/(Asce)Gt.1943-5606.0001694.

Jang, J., Cao, S.C., Stern, L.A., Jung, J. and Waite, W.F. (2018), "Impact of pore fluid chemistry on fine-grained sediment Fabric and compressibility", *J. Geophys. Res.-Solid Earth*, **123**(7), 5495-5514. https://doi.org/10.1029/2018jb015872.

Jang, J. (2022), "Influence of pore fluid chemistry on electrical force-dominated fabrics of fine-grained soils: implications in submerged sediments", *J. Korean Soc. Hazard Mitig.*, **22**(3), 151-158. https://doi.org/10.9798/KOSHAM.2022.22.3.151.

Kayabali, K. and Tufenkci, O.O. (2010), "Shear strength of remolded soils at consistency limits", *Can. Geotech. J.*, **47**(3), 259-266. https://doi.org/10.1139/T09-095.

Kennett, J. (1982), "Marine geology", Prentice-Hall, Inc. Englewood Cliffs, N.J.

Lambe, T.W., and Whitman, R.V. (1969), "Soil mechanics", John Wiley & Sons. New York.

Leonards, G.A. and Altschaeffl, M. (1964), "Compressibility of clay", *J. Soil Mech. Found. Division*, **90**(5), 133-156.

McBride, M.B. and Baveye, P. (2002), "Diffuse double-layer models, long-range forces, and ordering in clay colloids", *Soil Sci. Soc. Am. J.*, **66**(4), 1207-1217.

Mitchell, J.K. and Soga, K. (2005), "Fundamentals of soil behavior", John Wiley & Sons, Inc. New Jersey.

Oda, M. (1977), "Co-ordination number and its relation to shear strength of granular material", *Soils Found.*, **17**(2), 29-42. https://doi.org/10.3208/sandf1972.17.2_29.

Onyejekwe, S., Kang, X. and Louis, G. (2015), "Assessment of empirical equations for the compression index of fine-grained soils in Missouri", *Bull. Eng. Geol. Environ.*, **74**, 705-716. https://doi.org/10.1007/s10064-014-0659-8.

Reynolds, O. (1886), "Dilatancy", *Nature*, **33**(853), 429.

Rowe, P.W. (1962), "The stress-dilatancy relation for static equilibrium of an assembly of particles in contact", *P. R. Soc. A: Math. Phy.*, **269**(1339), 500-527. https://doi.org/10.1098/rspa.1962.0193.

Santamarina, J.C., Klein, K.A. and Fam, M.A. (2001), "Soils and waves", John Wiley & Sons. New York.

Schmertmann, J.H. (1991), "The mechanical aging of soils", *J. Geotech. Eng.*, **117**(9), 1288-1330. https://doi.org/10.1061/(ASCE)0733-9410(1991)117:9(1288).

Shariati, M., Azar, S.M., Arjomand, M.A., Tehrani, H.S., Daei, M. and Safa, M. (2020), "Evaluating the impacts of using piles and geosynthetics in reducing the settlement of fine-grained soils under static load", *Geomech. Eng.*, **20**(2), 87-101. https://doi.org/10.12989/gae.2020.20.2.087.

Sogami, I. and Ise, N. (1984), "On the electrostatic interaction in macroionic solutions", *J. Chem. Phys.*, **81**(12), 6320-6332. https://doi.org/10.1063/1.447541.

Taylor, D.W. (1948), "Fundamentals of soil mechanics", John Wiley&Sons, Inc. New York.

Terzaghi, K., Peck, R.B. and Mesri, G. (1996), "Soil mechanics in engineering practice", John Wiley & Sons, Inc. New York.

Thapa, K.B., Katti, K.S. and Katti, D.R. (2020), "Compression of Na-montmorillonite swelling clay interlayer is influenced by fluid polarity: A steered molecular dynamics study", *Langmuir*, **36**(40), 11742-11753. https://doi.org/10.1021/acs.langmuir.0c01412.

Tiwari, B. and Ajmera, B. (2011), "Consolidation and swelling behavior of major clay minerals and their mixtures", *Appl. Clay Sci.*, **54**(3-4), 264-273. https://doi.org/10.1016/j.clay.2011.10.001.

Tiwari, B. and Ajmera, B. (2012), "New correlation equations for compression index of remolded clays", *J. Geotech. Geoenviron. Eng.*, **138**(6), 757-762. https://doi.org/10.1061/(Asce)Gt.1943-5606.0000639.

Verwey, E.J.W., Overbeek, J.T.G. and Nes, K.V. (1948), "Theory

of the stability of lyophobic colloids; the interaction of sol particles having an electric double layer", Elsevier Pub. Co., xi, 205 p. p. New York.

Won, J., Park, J., Kim, J. and Jang, J. (2021), "Impact of particle sizes, mineralogy and pore fluid chemistry on the plasticity of clayey soils", *Sustainability*, **13**(21). ARTN 11741. https://doi.org/10.3390/su132111741.

Yang, Y. F., Qiao, R., Wang, Y. F. and Sun, S.Y. (2021), "Swelling pressure of montmorillonite with multiple water layers at elevated temperatures and water pressures: A molecular dynamics study", *Appl. Clay Sci.*, **201**. ARTN 105924. https://doi.org/10.1016/j.clay.2020.105924.

Young, H.D. and Freedman, R.A. (2004), "University physics", Pearson, San Francisco, CA.

Yu, Y., Wang, Z. and Sun, H.Y. (2020), "Optimal design of stone columns reinforced soft clay foundation considering design robustness", *Geomech. Eng.*, **22**(4), 305-318. https://doi.org/10.12989/gae.2020.22.4.305.

Zeng, L.L., Gao, Y.F. and Hong, Z.S. (2021), "Quantitative shear strength-consolidation stress-void ratio interrelations for reconstituted clays", *Geotechnique*, **71**(10), 843-852. https://doi.org/10.1680/jgeot.18.P.262.